International Journal of Mechanical Sciences 52 (2010) 602–611

Contents lists available at ScienceDirect

International Journal of Mechanical Sciences

journal homepage: www.elsevier.com/locate/ijmecsci

Shear behaviour of brick–mortar interface in CFRP retrofitted or repaired masonry

Bibiana Luccioni [a,*], Viviana C. Rougier [b]

[a] Structures Institute, National University of Tucumán, CONICET, Country Las Yungas, 4107 Yerba Buena, Tucumán, Argentina
[b] National Technological University/Reg. Fac. Concepción del Uruguay, Concepción del Uruguay, Argentina

ARTICLE INFO

Article history:
Received 3 October 2008
Received in revised form
22 December 2009
Accepted 22 December 2009
Available online 4 January 2010

Keywords:
Masonry
Fiber reinforced polymers
Retrofitting
Repair
Interface
Shear strength

ABSTRACT

There are many unreinforced masonry buildings all over the world. Many of them are located in seismic zones and are, therefore, susceptible to lateral forces caused by earthquakes. The transmission of these forces to the foundations is made through load bearing walls and depends on the shear strength and stiffness of masonry.

In plane shear strength of load bearing masonry walls depends on many factors like the bricks and mortar strength and the way the wall is constructed. It is mainly due to shear strength of the brick–mortar interface given by the adhesion and by the friction caused by normal compression loads. Under severe seismic loads the ultimate strength capacity of the interface is achieved and the structure collapses.

The results of an experimental program performed to study the shear behaviour of CFRP retrofitted and repaired masonry are presented in this paper. Increase of strength, ductility and stiffness due to the addition of CFRP laminas is specially analyzed. Specimens formed by three bricks and two mortar joints without reinforcement, retrofitted and repaired with CFRP laminas were tested under quasi-static and cyclic load.

Additionally, the numerical study of the same specimens is presented. The specimens were modelled with 2D and 3D finite elements programs. Orthotropic plasticity models were used for bricks and mortar, including brick–mortar interfaces and CFRP laminas. Experimental results were used to calibrate the parameters of the material models and a numerical tool for the mechanical analysis of retrofitted or repaired masonry panels was developed. A parametric numerical study was also carried out with these numerical models in order to obtain the optimal dimensions and orientation of the reinforcing bands.

1. Introduction

Masonry is a non-homogeneous composite anisotropic material made of hollow or solid bricks. The behaviour of masonry units is inelastic and complex even under very low load levels. The exact prediction of lateral load capacity of unreinforced masonry walls is not simple due to the complexity of the brick–mortar interaction [1]. The main in plane failure modes of unreinforced masonry walls under seismic loads can be summarized as follows [1].

Shear failure: This failure mode occurs when tension stresses generated in the wall under the combination of lateral and vertical loads, exceeds the tension strength of masonry. Before reaching maximum lateral load, diagonal cracks are developed. In case the bricks are relatively more resistant than the mortar, these cracks follow the way of horizontal and vertical joints or they can go through the bricks in the opposite case. The probability of this last situation increases with the value of vertical load and, in this case, failure can be explosive.

Sliding failure: This type of failure appears in case of low vertical loads or low friction coefficients that can be due to poor mortar quality. Cracks are initially formed in horizontal joints and can generate sliding planes extending to the complete length of the wall leading to the displacement of the upper part of the wall from the bottom part of it.

Flexure failure: This type of failure is attained for high flexion/shear ratios or in case shear strength has been improved. Failure is due to the crushing of compressed zones that causes the overturning of the wall.

This paper is focused on the second type of failure. In this case, the shear strength of masonry can approximately be estimated as follows [2]:

$$\tau_b = \tau_{bo} + \mu\sigma_N \quad (1)$$

* Corresponding author. Tel./fax: +54 381 43 64 087.
E-mail address: bluccioni@herrera.unt.edu.ar (B. Luccioni).
URL: http://www.herrera.unt.edu.ar/iest (B. Luccioni).

0020-7403/$ - see front matter © 2009 Elsevier Ltd. All rights reserved.
doi:10.1016/j.ijmecsci.2009.12.009

where τ_b is the shear strength of masonry; τ_{bo} is the bond shear strength of the brick–mortar interface (shear strength in absence of normal loads); μ is the brick–mortar friction coefficient and σ_N is the normal stress. In absence of normal stress, the shear strength of the brick–mortar interface is the main factor dominating failure. In presence of severe seismic loads, this strength can be exceeded. Efficient and safe retrofitting and repairing techniques are needed in these cases.

Several reinforcing and retrofitting methods for masonry walls have been studied in recent years. The addition of frame elements to reduce the loads on the walls or surface treatments, such as cement infill to increase the strength and ductility of the walls, are usually required. These retrofitting techniques often add a significant mass to the structure, require high execution time and costs and are not reliable in many cases [3]. Studies performed after the Northridge Earthquake (1994) showed that 450 buildings reinforced before the earthquake failed after it [4].

Consequently, the study of new materials and techniques for the efficient retrofitting of damaged masonry structures is extremely necessary. Recent advances in the field of polymeric fiber reinforced composites (FRP) materials have led to the development of new materials potentially efficient for the retrofitting of masonry structures in areas where conventional materials have failed [3]. Research activities developed by different authors [4–19] have shown that polymer reinforced composites give a light and efficient alternative to traditional materials and improve the behaviour of masonry elements under monotonic, seismic and explosive loads.

From the structural point of view, dynamic properties of the structure are not altered since the added mass and stiffness are negligible. This fact is of fundamental importance for the reinforcement of structures that could be subjected to moderate or severe earthquakes, since any increase of mass or stiffness indefectibly leads to an increase of seismic forces. This system has also been proved efficient for the retrofitting of damaged historical masonry buildings [7].

The efficiency of this retrofitting system under static, cyclic, pseudo-dynamic and dynamic loads has been confirmed by different studies [6,2,4].

According to recent research by El-Dakhakhni et al. [17] on small masonry specimens made with hollow concrete blocks subjected to uniaxial compression normal to the bed joint, the reinforcement with fiber reinforced polymeric composites not only increases the strength but also increases the ductility preventing out of plane brittle failure and keeping the wall integrity.

The external reinforcement of masonry elements with polymeric fiber reinforced composite materials has also proved to increase ductility and strength and prevent brittle failure of masonry panels under compression parallel to the bed joints [17].

Shear reinforcement of masonry walls with fiber reinforced polymers has also been studied. Valluzzi et al. [20] developed an experimental program to investigate the efficiency of this type of reinforcement. They assessed the performance of different types of composites and reinforcement schemes of solid bricks masonry panels subjected to diagonal compression. El-Dakhakhni et al. [17] tested small hollow concrete brick masonry panels without reinforcement and reinforced with glass fiber reinforced polymers. Gabor et al. [18] experimentally studied the in plane shear behaviour of hollow clay brick masonry panels reinforced with glass fiber reinforced polymers and carbon fiber reinforced polymers.

From the results obtained by Gabor et al. [18] and Valluzzi et al. [20] it can be concluded that fiber reinforced polymer reinforcement increases shear strength and ductility depending on the reinforcement scheme. It also increases the stiffness, especially in masonry panels made by solid bricks, and prevents brittle failure only for total reinforcement [18]. Eshani et al. [2] investigated the efficiency of external shear reinforcement of small specimens made by three solid bricks and two joints. The experimental results showed that strength and ductility were increased. Fiber orientation significantly affects the stiffness but not the strength. The increase of anchorage length leads to greater strength.

One of the first experimental studies to improve the strength masonry walls was performed by Schwegler [4] who tested a full scale one floor building.

Many researchers have also studied the seismic reinforcement of masonry panels with fiber reinforced polymers [1,21]. It was observed that the reinforcement improves lateral stability of the walls.

Other authors [3,9–15] also studied the efficiency of fiber reinforced polymers to improve ductility and strength under out of plane load of masonry walls and beams.

Some recent research has focused on the study of the blast strength of masonry walls reinforced with fiber reinforced polymers. In this case, the reinforcement increases the structure strength and reduces fragmentation. This property is very attractive since fragmentation is the principal cause of damage in a blast event [22].

Although efficiency of retrofitting techniques using fiber reinforced composite materials has been experimentally proved, a better description of the mechanical behaviour of reinforced masonry under different load conditions should be obtained in order to improve intervention techniques. It is difficult to obtain reinforcing and/or retrofitting effective criteria that cover strength, stiffness, ductility, durability and bond criteria from available theories and design methods usually used in engineering practice.

On the other side, although retrofitting of damaged masonry structures is of fundamental importance [23–28], not enough research work concerning the behaviour of damaged masonry repaired with fiber-reinforced polymers can yet be found in the open literature.

The objectives of this paper are the analysis of the main features of in-plane shear behaviour of brick–mortar interface, the assessment of the retrofitting/repairing with carbon fiber reinforced polymers CFRP and the calibration of a numerical tool useful for the simulation of the interface behaviour. The experimental and numerical results presented in this paper could help the understanding of new resistant mechanisms introduced by the reinforcement. In this sense, the paper represents a contribution to the development of reinforcing or retrofitting criteria.

2. Test description

2.1. Introduction

The behaviour of small specimens made of three bricks and two mortar joints (triplets) under shear was experimentally studied. The tests were mainly similar to those proposed in the European Standard prEN 1052-3 Part 3 [29] to minimize flexure. The central brick was displaced about 86.7 mm (one third of the bricks longest side) in order to model masonry structures. Unreinforced, retrofitted and repaired specimens were tested using different carbon fiber reinforced polymers (CFRP) configurations.

As a sudden failure was expected to occur, the tests were performed under monotonic increasing or cyclic load with displacement control with low rate (0.004 mm/s).

The mechanical characteristics of the mortar used are presented in Table 1 in which the dimension refers to mortar thickness. The ultimate strength values correspond to the mean of 20 half test specimen of $40 \times 40 \times 160\,[mm^3]$. The mean values of the strength, elasticity modulus and Poisson ratio for the two types of bricks used in the tests are also presented in Table 1 together with the dimensions of the bricks.

Unidirectional carbon fibers fabric (Sika Wrap Hex 103 C) was used for the reinforcement and retrofitting of masonry elements. This fiber fabric has high content of carbon and presents high modulus and strength. In all specimens the fiber fabric was saturated in situ with epoxy system Sikadur Hex 300. The properties of the lamina are obtained from specifications by the manufacturer and presented in Table 2.

In order to remove mortar remains and dust, the surfaces of the panel were carefully cleaned with a steel brush and high pressure air. The carbon fiber fabric soaked up with the epoxy resin was applied to the front and back sides of the specimen previously soaked with the same resin. In all cases, one lamina of 1 mm final thickness was applied to the front and back sides of the specimen with the fibers normal to the mortar joints.

Table 1.
Mortar and bricks mechanical properties.

Properties	Mortar	Bricks
Elasticity modulus E (MPa)	1528	1400
Compression ultimate strength, σ_{uc} (MPa)	4	8.28
Poisson ratio, ν	0.21	0.15
Dimensions (mm)	15	$260 \times 125 \times 55$

Table 2.
Mechanical properties of carbon fiber reinforced epoxy lamina.

Elasticity modulus E (MPa)	72500
Tension strength, σ_t (MPa)	960
Poisson ratio, ν	0.2
Ultimate tension strain (%)	1.33
Thickness (mm)	1

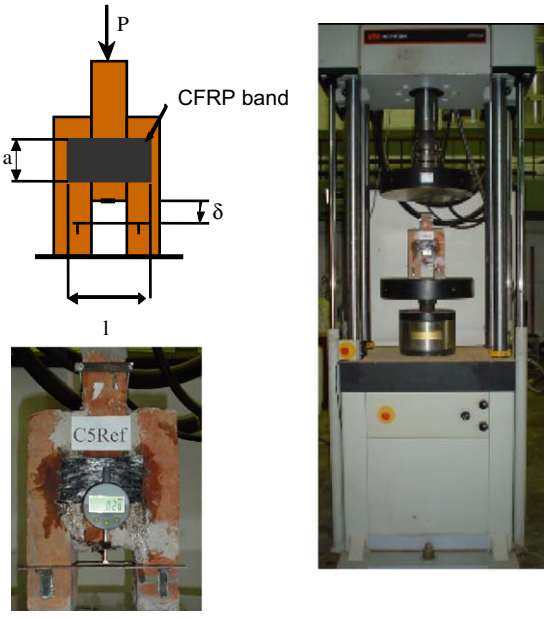

Fig. 1. Load and test setup.

The tests and measurement setup are illustrated in Fig. 1. A summary of the set of specimens tested is presented in Table 3. In order to obtain the optimum dimensions of the CFRP bands both width and length were varied as specified in Table 3.

The load–displacement curves obtained for retrofitted specimens (C4Ret, C5Ret, C6Ret, C7Ret) and the comparison with those for unreinforced specimens (C1, C2, C8, C9) are presented in Fig. 2. The ultimate strength and ductility were strongly increased by this retrofitting technique. It is clear that the strength improvement provided by the CFRP is dependent on the band dimensions, especially on its anchorage length.

The total stiffness was practically not modified. Although the lamina stiffness is very high in comparison with masonry stiffness, its contribution is limited to the thickness of the composite that represents only 1.5% of the total width of the retrofitted specimen.

Load-displacement curves for previously damaged and later repaired specimens (C1Rep, C2Rep, C8Rep, C9Rep) are presented in Fig. 3, together with the curves corresponding to unreinforced specimens (C1, C2, C8, C9). Unreinforced triplets exhibited a brittle failure. The specimen repaired with the largest band recovered and even increased original shear load capacity. On the contrary, the specimen repaired with the smallest band could not recover its load capacity. Nevertheless, a significant ductility increase was evidenced by the failure mode for both cases. None of the repaired specimens recovered the original stiffness.

Additionally, two specimens (CC3 and CC6) were tested under cyclic load. The load displacement curve for four load cycles is compared to that of the monotonic increasing load in Fig. 4a. An important loss of strength and stiffness degradation is observed for the cyclic load.

Specimen CC3 was repaired later with CFRP bands and subjected to the same type of load. The load displacement curve is shown in Fig. 4b. The load capacity was increased over the initial one and an important increase in ductility was obtained. Stiffness was barely modified.

The ultimate load values for all these tests are included in Table 3. The different failure modes obtained from the tested triplets are illustrated in Fig. 5. Specimens without reinforcement exhibited a very brittle failure with abrupt sliding of joints. In the case of the specimens tested under cyclic load, failure mode was similar but even more sudden.

The same failure mechanism was observed by Abdoud et al. [30] for triplets tested under cyclic load and low values of compression normal to the bed joint. For high values of compression, failure was quasi-brittle with failure of bricks and joints.

Repaired and retrofitted specimens exhibited a more ductile failure caused by the brick's failure in the CFRP bands anchorage zone that produced the pull out of the bands.

In general, it can be concluded that both strength and ductility are improved when specimens are retrofitted or repaired. The length of the CFRP bands is decisive in the increase of strength and ductility.

A significant increment in strength and ductility of triplets retrofitted with GFRP bands was also found by Eshani et al. [2]. They did not take into account the contribution of mortar joints since they replaced them by two wood boards in order to prove the efficiency of this repair method when the joints have no strength. Eshani et al. [2] also observed an increase in strength for longer bands. They also found that, in order to improve ductility, the best orientation of fibers is normal to the load.

Table 3.
Triplets tested.

Specimen	Type of test	Retrofitting/Repairement	$P_{máx.}$ (*k*N)
C1	Quasi-static increasing load	————————————	8.97
C2	Quasi-static increasing load	————————————	9.99
CC3	Quasi static cyclic load-unloading	————————————	5.14
C4Ret	Quasi-static increasing load	Retrofitted with $120 \times 90\,[mm^2]$ bands	22.67
C5Ret	Quasi-static increasing load	Retrofitted with $100 \times 54\,[mm^2]$ bands	14.96
C1Rep	Quasi-static increasing load	C1 repaired with $120 \times 90\,[mm^2]$ bands	17.52
C2Rep	Quasi-static increasing load	C2 repaired with $100 \times 54\,[mm^2]$ bands	6.51
CC3Rep	Quasi-static cyclic load	CC3 repaired with $120 \times 90\,[mm^2]$ bands	12.00
C6Ret	Quasi-static increasing load	Retrofitted with $140 \times 80\,[mm^2]$ bands	23.00
C7Ret	Quasi-static increasing load	Retrofitted with $140 \times 80\,[mm^2]$ bands	16.10
C8	Quasi-static increasing load	————————————	5.18
C9	Quasi-static increasing load	————————————	3.93
C8Rep	Quasi-static increasing load	C8–C9 repaired with $140 \times 80\,[mm^2]$ bands	10.53
C9Rep	Quasi-static increasing load	C8–C9 repaired with $140 \times 80\,[mm^2]$ bands	6.71

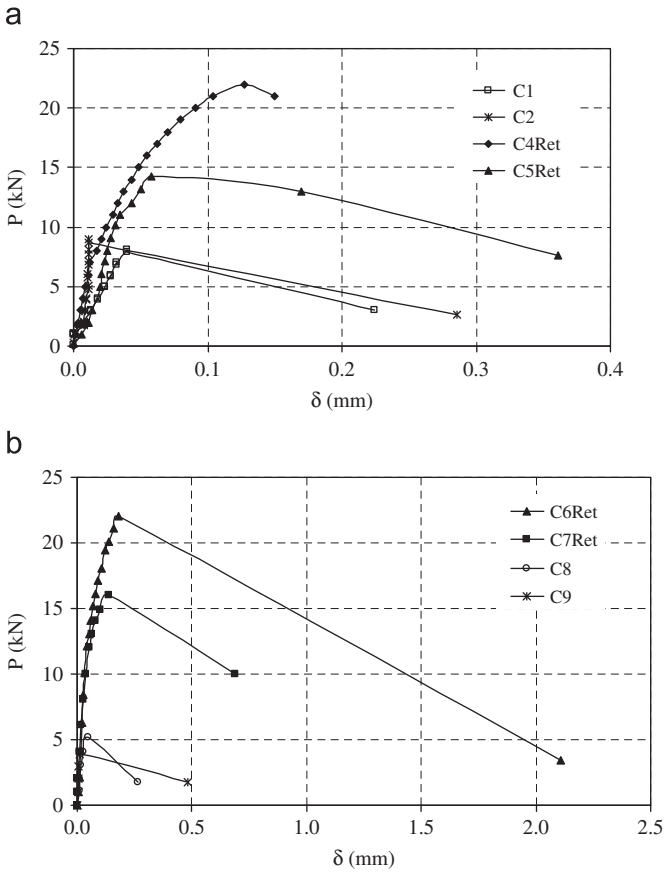

Fig. 2. Load displacement curves for unreinforced specimens and retrofitted specimens: (a) C1, C2, C3Ret and C4Ret; (b) C8, C9, C6Ret and C7Ret.

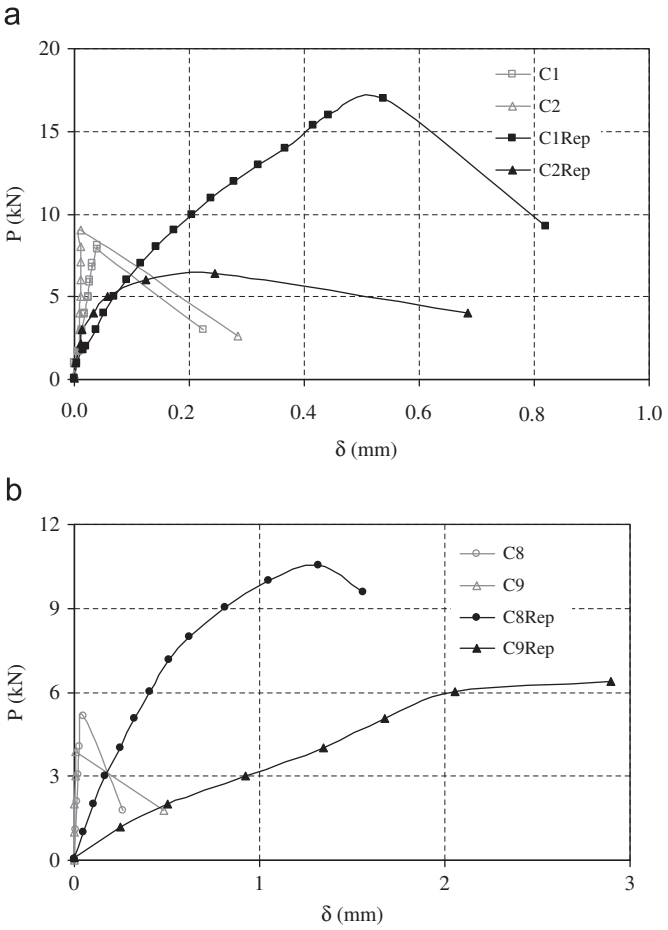

Fig. 3. Load displacement curves for unreinforced specimens and previously damaged and later reinforced specimens: (a) C1, C2, C1Rep and C2 Rep; (b) C8, C9, C8Rep and C9Rep.

3. Numerical analysis

3.1. Introduction

In order to study the behaviour of the brick–mortar interface of unreinforced, retrofitted and repaired specimens, and to calibrate a numerical tool for the analysis of this type of problem, all the specimens tested were modelled using finite element method. 2D and 3D non-linear finite element programs developed by the authors for research purposes were used. Numerical results were compared with experimental ones.

Taking into account the symmetry of the problem, only one half of them was modelled. The load and test setup is shown in Fig. 6a. Triangular plane stress elements with three nodes were used for most of the simulations but, in order to reproduce the debonding of the CFRP laminas, some simulations were carried out with three-dimensional models using tetrahedral elements with four nodes. The different meshes used for unreinforced and retrofitted or repaired specimens under plane stress are presented in Figs. 6b and 6c. Fig. 6d shows shear stress contours in bricks

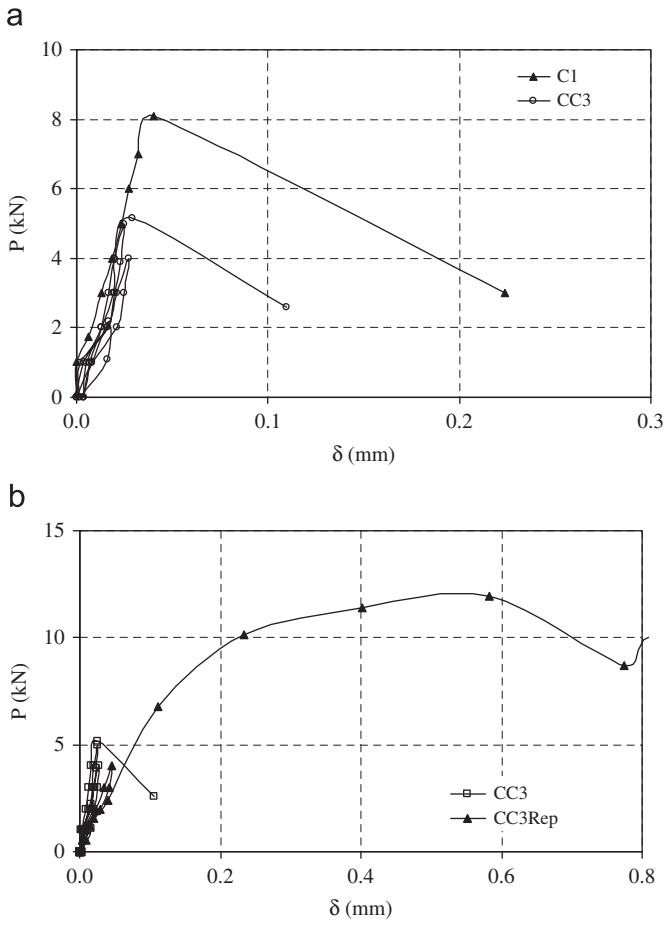

Fig. 4. Load displacement curves for cyclic tests: (a) unreinforced specimens; (b) repaired specimen.

and mortar for a repaired specimen near failure. The 3D mesh used for a retrofitted specimen is presented in Fig. 7a while the 3D deformed mesh is illustrated in Fig. 7b.

3.2. Constitutive models

A fine meshing of bricks and mortar was defined. An orthotropic plastic model was used both for bricks and mortar [31,32], with different values for the material constants in correspondence with material mechanical properties. In the case of retrofitted or repaired specimens modelled in plane stress, the sets of brick and CFRP lamina or mortar and CFRP lamina, were modelled with classical "mixture theory" (Voigt model) [33,34]. In this simplified composite model all the components are assumed to have the same strains and the composite stress is obtained as the sum of the component stresses multiplied by their respective volume fractions. A general orthotropic elastoplastic model [35] was used for the CFRP lamina. As the mechanical properties provided by the manufacturer were not enough to complete the description of the material and it was not simple to test the lamina due to its extremely reduced thickness, the rest of the mechanical properties were obtained with a generalization of mixture theory for composite laminates developed by one of the authors [33,34].

The orthotropic model used is based on the assumption that two spaces can be defined [36,37]: (a) a real anisotropic space and (b) a fictitious isotropic space. The problem is solved in the fictitious isotropic space allowing the use of elastoplastic models originally developed for isotropic materials. The isotropic elastoplastic model used in this paper includes energy-based criteria to make it suitable for brittle materials [24].

Stress tensors in both spaces are related to a tensor transformation that can be written as

$$\boldsymbol{\tau} = \boldsymbol{A}(\boldsymbol{\sigma}, \kappa^p) : \boldsymbol{\sigma} \tag{2}$$

where $\boldsymbol{\tau}$ and $\boldsymbol{\sigma}$ are the stress tensors in spaces (a) and (b), respectively; and $\boldsymbol{A}$ is a fourth order transformation tensor that contains the information about strength anisotropy depending on material symmetry. In the most general case, this tensor varies with the stress state and the evolution of the inelastic process represented by the isotropic plastic hardening variable κ^p [31]. In this paper, all the component materials were assumed initially isotropic or orthotropic with 3 axes of material symmetry. There are different alternatives to define tensor $\boldsymbol{A}$ for this case [37–41]. The simplest way is a diagonal fourth order tensor [34]

$$A_{ijkl} = \sum_{m=1}^{3}\sum_{n=1}^{3} \delta_{im}\delta_{jn}\delta_{km}\delta_{ln}\overline{\tau}/\overline{\sigma}_{mn} \tag{3}$$

where $\overline{\tau}$ is the strength in the fictitious isotropic space and $\overline{\sigma}_{mn}$ is the actual strength in the direction m in the plane with normal $\boldsymbol{n}$. A better approach has been proposed by Oller et al. [41].

The plastic threshold is defined through a yielding function

$$F(\boldsymbol{\sigma}; \alpha) = \overline{F}(\boldsymbol{\tau}; \overline{\alpha}) = 0 \tag{4}$$

where F and $\overline{F}$ represent the yielding function in the real anisotropic space and the fictitious isotropic space, respectively; α and $\overline{\alpha}$ are plastic internal variables in correspondence with both spaces.

The transformation defined by Eq. (2) allows the use of yielding functions $\overline{F}$ defined for isotropic materials in the fictitious isotropic space. It should be noted that this space is isotropic with respect to yielding thresholds and strength but not necessarily with respect to other properties like elastic stiffness.

The constitutive equation for an elastoplastic material can be written as follows:

$$\boldsymbol{\sigma} = \boldsymbol{C} : \boldsymbol{\varepsilon}^e = \boldsymbol{C} : (\boldsymbol{\varepsilon} - \boldsymbol{\varepsilon}^p) \tag{5}$$

where $\boldsymbol{C}$ is the elastic stiffness tensor, $\boldsymbol{\varepsilon}^e$ is the elastic strain tensor, $\boldsymbol{\varepsilon}$ is the strain tensor and $\boldsymbol{\varepsilon}^p$ is the plastic or inelastic strain tensor.

Evolution of plastic strain in real space is defined with the well-known flow rule

$$\dot{\boldsymbol{\varepsilon}}^p = \dot{\lambda}(\partial G/\partial \boldsymbol{\sigma}) \tag{6}$$

where G is the plastic potential function defined in the real stress space. Instead of working with this function that should be anisotropic, function $\overline{G}$ defined in the fictitious isotropic space could be used.

$$G(\boldsymbol{\sigma}, \alpha) = \overline{G}(\boldsymbol{\tau}, \overline{\alpha}) \tag{7}$$

Eq. (6) can then be rewritten as

$$\dot{\boldsymbol{\varepsilon}}^p = \dot{\lambda}(\partial \overline{G}/\partial \boldsymbol{\sigma}) = \dot{\lambda}(\partial \overline{G}/\partial \boldsymbol{\tau}) : (\partial \boldsymbol{\tau}/\partial \boldsymbol{\sigma}) = \dot{\lambda}(\partial \overline{G}/\partial \boldsymbol{\tau}) : \boldsymbol{A} = \dot{\boldsymbol{\lambda}}\overline{\mathbf{h}} \quad \text{with } \boldsymbol{A} = \partial \boldsymbol{\tau}/\partial \boldsymbol{\sigma} \text{ and } \overline{\mathbf{h}} = (\partial \overline{G}/\partial \boldsymbol{\tau}) : \boldsymbol{A} \tag{8}$$

where $\overline{\mathbf{h}}$ is a second-rank tensor and represents the plastic flow in the real orthotropic space.

3.3. Numerical results

The load-relative displacement δ curves obtained for unreinforced triplets and their comparison with experimental results are presented in Fig. 8. The displacement δ represents the relative displacement between the bottom face of the central brick and a fixed point in lateral bricks. A reasonable global agreement

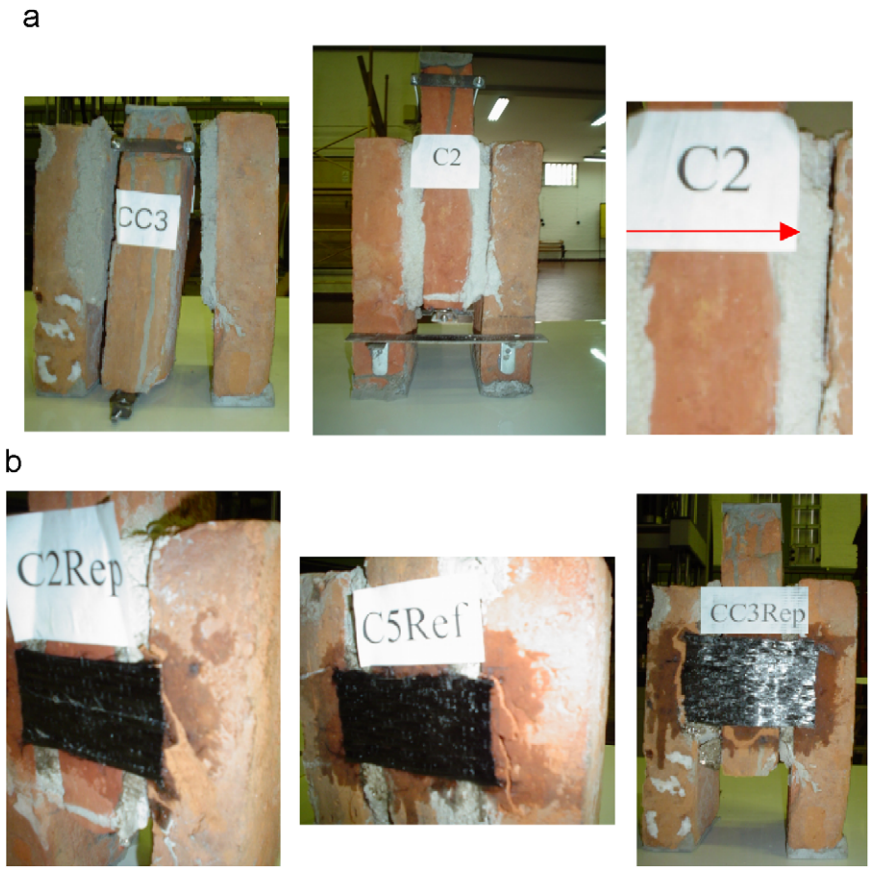

Fig. 5. Failure modes for tested triplets: (a) unreinforced specimens; (b) repaired and retrofitted specimens.

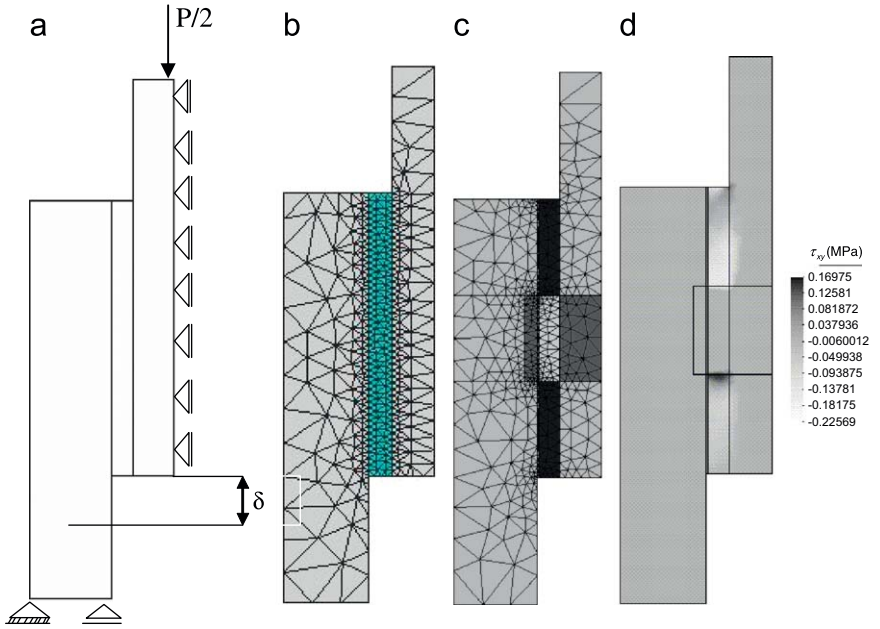

Fig. 6. Finite element models: (a) load and boundary conditions; (b) 2D finite element mesh for an unreinforced specimen; (c) 2D finite element mesh for a repaired specimen; (d) shear stress contours in bricks and mortar for a repaired specimen.

between numerical and experimental results can be observed in Fig. 8. Nevertheless, the maximum load and energy dissipation were overestimated. Experimental failure is very brittle with sudden sliding of the central brick due to the failure of the brick–mortar interface. This great discontinuous phenomenon can only be approximately modelled through the finite element model in which perfect bond between bricks and mortar was assumed and where this phenomenon is smeared in a finite width.

The load–displacement curves obtained for the retrofitted specimens and their comparison with experimental results are

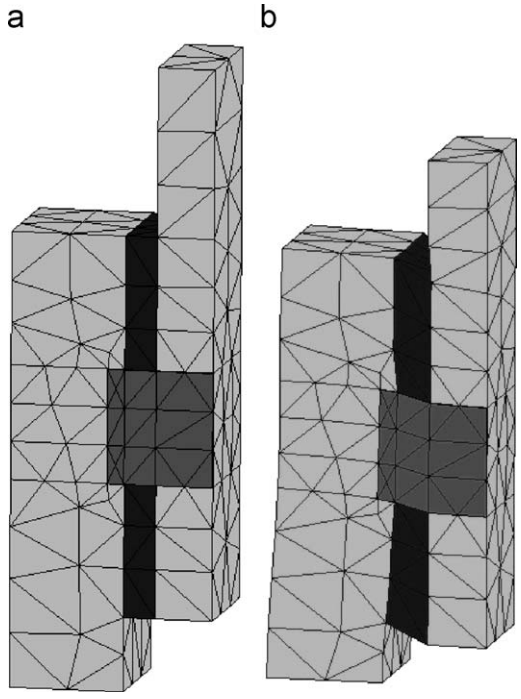

Fig. 7. 3D finite element mesh for a retrofitted specimen: (a) undeformed mesh and (b) deformed mesh.

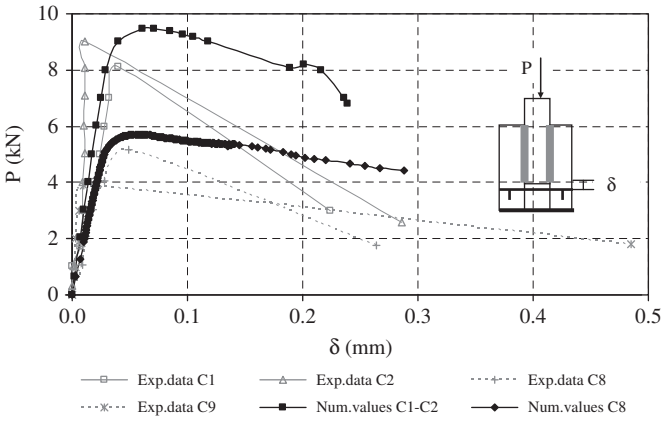

Fig. 8. Load displacement curves for unreinforced specimens. Numerical and experimental results.

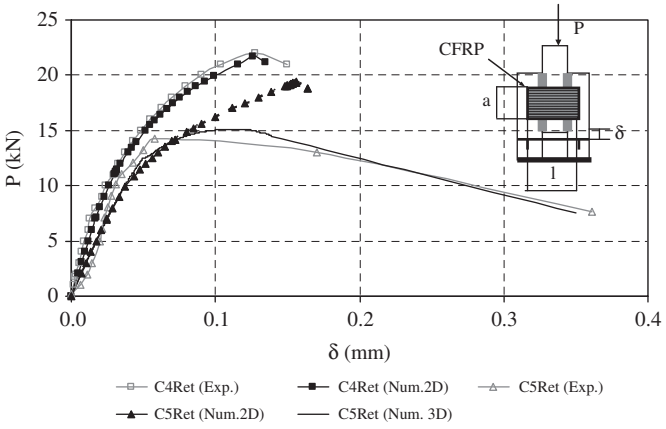

Fig. 9. Load displacement curves for retrofitted specimens. Numerical and experimental results.

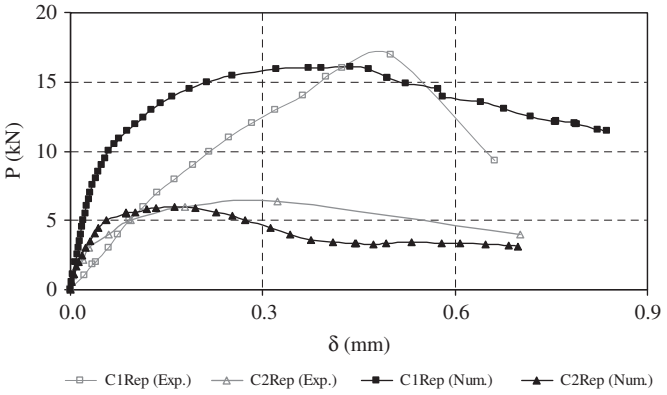

Fig. 10. Load displacement curves for repaired specimens. Numerical and experimental results.

presented in Fig. 9. It can be seen that the numerical model simulates the behaviour of the triplet retrofitted with the longer band (C4Ret) approximately but it is not able to simulate the brittle failure of C5Ret, retrofitted with shorter CFRP bands. The curve corresponding to numerical results over the failure load is represented with a dot line in Fig. 9. In this case, the failure was produced by the failure of the brick–CFRP lamina interface. This phenomenon cannot be reproduced with a two dimensional model.

Taking into account the above observations, this test was simulated again using a three-dimensional finite element model as that shown in Fig. 7a. The weakness of the brick–CFRP lamina interface was taken into account in the orthotropic constitutive model of the CFRP lamina using a reduced value of shear strength in the corresponding plane. In this way, the shear failure of the brick–CFRP lamina can be reproduced.

The load–displacement curve obtained with the three-dimensional model is included in Fig. 9. This model is able to reproduce the type of failure observed in the tests. Failure is defined by debonding of the brick–CFRP lamina interface when shear adhesion strength is achieved. In this three-dimensional model shear adhesion strength is represented by the shear strength of the composite lamina.

The behaviour of damaged specimens later repaired and reloaded to failure was also reproduced. The finite element models used in this case were similar to those used for retrofitted specimens. But, in order to reproduce the previous damage, a thin band of mortar, with reduced strength and stiffness according to previous results, was modelled in the brick–joint interface.

The load–displacement curves obtained and their comparison with experimental results are presented in Fig. 10. The numerical model reasonably reproduced the non-linear behaviour observed in the tests for the model repaired with the smaller band but it did not give a good fitting for the bigger CFRP band. Other numerical simulations carried out by Eshani et al. [2] with finite element programs could not reproduce experimental results either.

4. Parametric study

A parametric study performed on the same specimen as the one tested in the preceding section but repaired with CFRP bands of different length, width and orientation is presented in this section.

The influence of the CFRP band length was first analyzed. Four band lengths, 100, 120, 140 and 187 mm, were studied while width remains constant. The load–displacement curves obtained

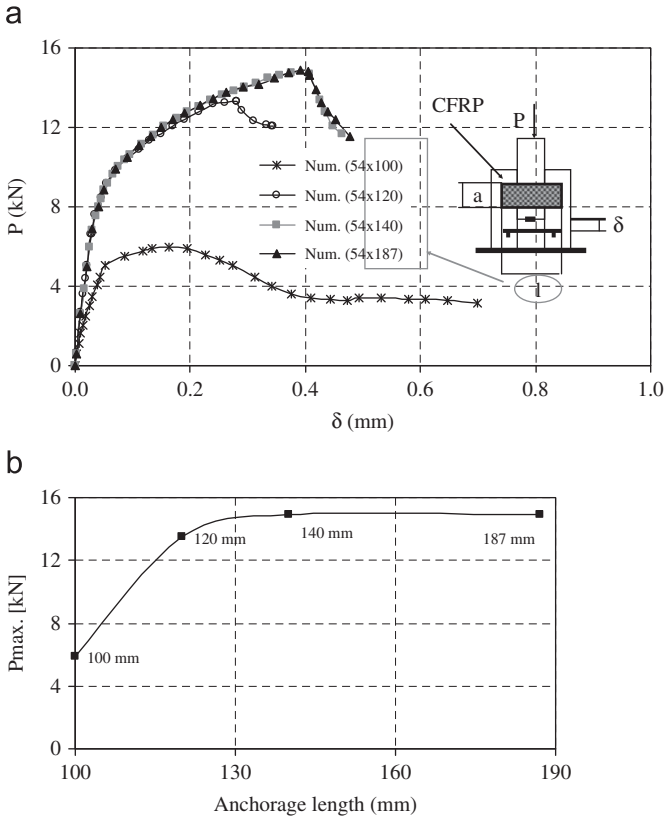

Fig. 11. Influence of band length: (a) load–displacement curves for different band length and (b) variation of maximum load capacity with CFRP band length

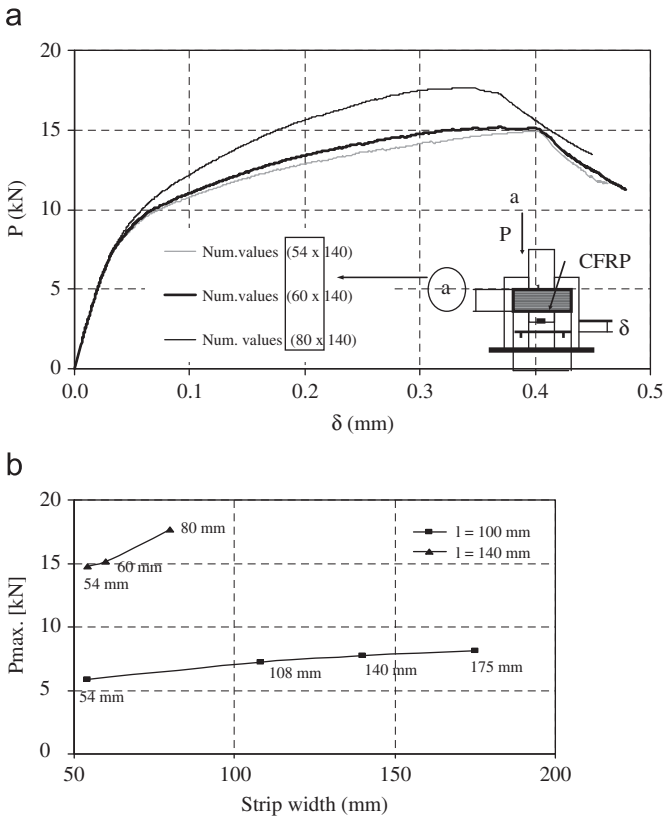

Fig. 12. Influence of band width: (a) load–displacement curves for different band width and (b) variation of maximum load capacity with CFRP band width for different band length.

for the different band lengths are presented in Fig. 11a. It shows that shear strength grows with the increase in band length up to a certain band length. For longer bands, there is practically no increase in ultimate shear strength. This can be easily appreciated in Fig. 11b where the maximum load is represented as a function of the anchorage length. From approximately 140 mm of band length the strength remains nearly constant.

Next, the CFRP band width was varied while the length remains constant. The corresponding load–displacement curves are presented in Fig. 12a where it is shown that the CFRP band width has practically no influence on the ultimate load capacity. The variation of strength as a function of CFRP band width for two different band lengths is presented in Fig. 12b. It can be seen that the band length significantly influences the strength. For 100 mm of band length the ultimate load is practically constant for different bands width. While for longer bands, an increase in ultimate load is obtained when the band width is increased. According to these remarks, it would be possible to find optimum band dimensions that allow improving the behaviour of damaged specimens with a low cost/benefit ratio.

Another variable to be analyzed was the orientation of the composite fibers with respect to the load direction or the bed joints. For this study the complete specimen was modelled. The finite element mesh used is illustrated in Fig. 13a. Load–displacement curves for different orientations of the composite are also presented in Fig. 13a. The maximum load capacity as a function of the angle of the fibers with respect to the load direction is presented in Fig. 13b. It can be seen that the strength is increased with the angle of the fibers and the behaviour is more linear. The maximum strength is obtained when the composite is placed with the fibers forming an angle of 30° with load direction.

The use of bidirectional CFRP laminas with different orientations of the fibers to repair previously damaged triplets was also studied. The load–displacement curves obtained for this case are

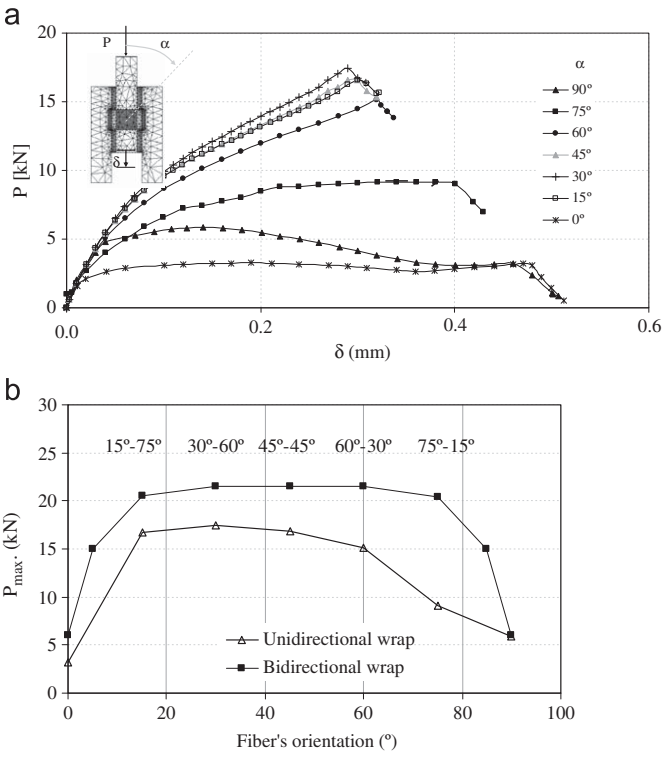

Fig. 13. Influence of fibers' orientation. (a) load–displacement curves for different band orientation and (b) variation of maximum load capacity with CFRP band fibers' orientation respect to load direction.

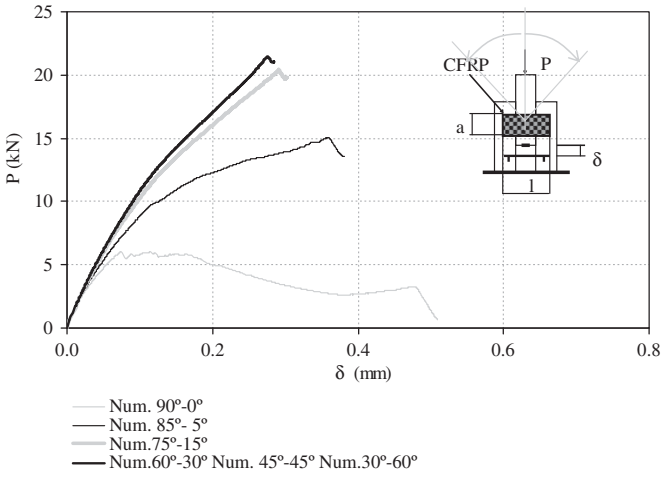

Fig. 14. Load–displacement curves for triplets repaired with different CFRP bidirectional band orientations respect to load direction.

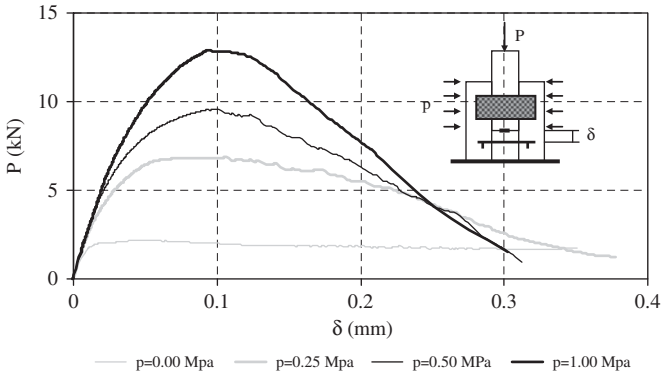

Fig. 15. Load–displacement curves for unreinforced triplets under different confinement pressures.

presented in Fig. 14. A marked strength increase is observed for low orientations (85–5°). The behaviour tends to be linear with the increase in the angle of orientation. The ultimate load capacity is almost the same for the angles 60–30°, 45–45° and 30–60°. The variation of ultimate load capacity for triplets repaired with bidirectional and unidirectional CFRP composites with different orientations is presented in Fig. 13b. It can be observed that greater loads can be attained in specimens repaired with bidirectional composite, for which there is practically no variation of strength with fiber orientation within certain inclination range.

Finally, the effect of confinement on shear behaviour of unreinforced and retrofitted triplets was numerically studied. For this purpose, the triplets were previously loaded with a compression load normal to the bed joint as shown in Figs. 15 and 16. Figs. 15 and 16 present the load-displacement curves obtained for the unreinforced and retrofitted specimens, respectively. The retrofitted triplets correspond to 54 mm × 100 mm CFRP bands orthogonal to load direction. As expected (see Eq. (1)), the triplet shear strength increases with the increase in confinement load. The effect of normal load is greater in the case of unreinforced specimens. In this case, shear strength is mainly due to shear strength of the mortar–brick interface. Comparing Figs. 15 and 16 it can be shown that, for high confinement pressures, the improvement in shear behaviour due to the CFRP retrofitting is practically negligible.

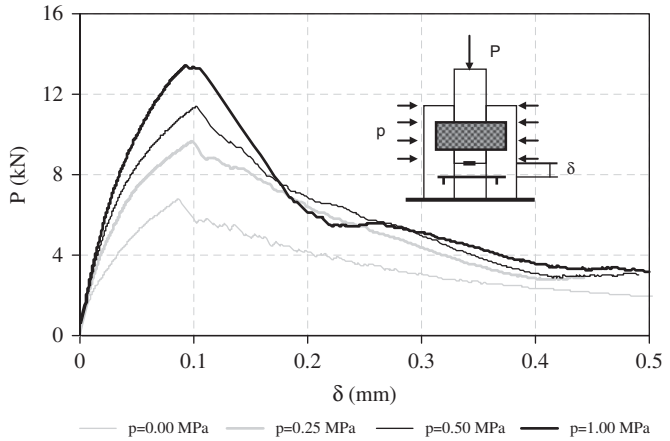

Fig. 16. Load–displacement curves for retrofitted triplets under different confinement pressures.

5. Conclusions

From the analysis and comparison of experimental and numerical results and from the parametrical study performed, the following conclusions can be stated.

The failure of unreinforced specimens under shear loads without normal compression is produced by sliding of the mortar joints and it is both brittle and sudden.

Depending on the dimensions of the bands used, the retrofitting with CFRP improves this brittle behaviour of the joints, preventing the sliding and increasing the ultimate strength.

The retrofitting with unidirectional CFRP bands oriented orthogonal to the joints increases the shear strength. The anchorage length of the CFRP band is a very important variable in the design of the shear reinforcement. Strength increases with the length of the bands. In general, the failure is produced by the failure of the bricks surface producing the debonding of the CFRP laminas.

Although repairing with CFRP composites does not allow recovering the initial stiffness, an improvement in shear capacity and ductility is achieved and the type of failure is modified.

In the case of specimens previously damaged and then repaired with CFRP bands orthogonal to the loading direction, shear capacity is not only recovered but also increased. The bands anchorage length is also a fundamental design value in this case. For specimens repaired with short bands the ultimate load capacity cannot be recovered but, in all cases, a ductility improvement is observed and is also manifested in the type of failure, similar to that observed in the case of retrofitted specimens. The orientation of the fibers with respect to the loading direction is important too. The greater increase is achieved for an angle of 30° for which the response tends to be linear. If a bidirectional composite is used for repairing, the influence of fiber orientation on strength improvement is more important.

The numerical model developed for retrofitted or repaired masonry using continuous models and classical mixture theory (Voigt Model) in two dimensions gives a reasonable simulation of the behaviour of the set of materials. It has the advantage of avoiding the discretization of the composite as a third material, reducing the computational cost and making parametrical studies easier.

When the debonding of the CFRP laminas should be modelled, a three-dimensional analysis should be performed. This type of study allows reproducing the failure by debonding of the

composite bands with reasonable approximation and to obtain a more accurate value of the ultimate load capacity.

Acknowledgments

The financial support of CONICET, CIUNT (National University of Tucumán) and Technological University is gratefully acknowledged. The authors also wish to thank Eng. Jorge Rendón and Eng. Paulino Maldonado, from Sika Colombia and Sika Argentina for donating the composite material used to carry out experimental tests and the collaboration of Ms. Amelia Campos in the English revision.

References

[1] ElGawady M, Lestuzzi P, Badoux M. Shear strength of URM walls retrofitted using FRP. Eng Struct 2006;28:1658-70.
[2] Ehsani M, Saadatmanesh H, Al-Saidy A. Shear behavior of URM retrofitted with FRP overlays. J Compos Constr 1997;1(1):17–25.
[3] Saadatmanesh H. Extending service life of concrete and masonry structures with fiber composites. Constr Build Mater 1997;11:327–35.
[4] ElGawady M, Lestuzzi P, Badoux M. Aseismic retrofitting of unreinforced masonry walls using FRP. Compos. Part B: Engng 2006;137:148-62.
[5] Bradley J, Christensen J, Gilstrap J, Dolan CH. Composite materials reinforcement of existing masonry walls. J Arch Eng 1996;2(2):63–70.
[6] Marshall O, Sweeney J, Trovillion J. Seismic rehabilitation of unreinforced masonry walls. ACI SP 1999;188:287–96.
[7] Luciano R, Sacco E. Damage of masonry panels reinforced by FRP sheets. Int J Solids Struct 1998;35:1723–41.
[8] Ehsani M, Saadatmanesh H, Velazquez-Dimas J. Behavior of retrofitted URM walls under simulated earthquake loading. J Compos Constr 1999;3:134–42.
[9] Velazquez-Dimas J, Eshani M. Modeling out-of plane behavior of URM walls retrofitted with fiber composites. J Compos Constr 2000;4:172–81.
[10] Albert M, Elwi A, Cheng J. Strengthening of unreinforced masonry walls using FRPs. J Compos Constr 2001;5:76–84.
[11] Hamilton III H, Dolan C. Flexural capacity of glass FRP strengthened concrete masonry walls. J Compos Constr 2001;5:170–8.
[12] Hamoush S, Mcginley M, Mlakar P, Scott D, Murray K. Out-of plane-strengthening of masonry walls with reinforced composites. J Compos Constr 2001;5:139–45.
[13] Hamoush S, Mcginley M, Mlakar P, Terro M. Out-of plane-behavior of surface-reinforced masonry walls. Constr Build Mater 2002;16:341–51.
[14] Tumialan J, Galati N, Nanni A. Field assessment of unreinforced masonry walls strengthened with fiber reinforced polymer laminates. J Struct Eng 2003;129:1047–56.
[15] Tan K, Patoary M. Strengthening of masonry walls against out-of-plane loads using fiber-reinforced polymer reinforcement. J Compos Constr 2004;8: 79–87.
[16] Ehsani M, Saadatmanesh H. Seismic retrofit of URM walls with fiber composites. TMS Journal 1996;14:63-72.
[17] El-Dakhakhni W, Hamid A, Hakam Z, Elgaaly M. Hazard mitigation and strengthening of unreinforced masonry walls using composites. Compos Struct 2005;73:458–77.
[18] Gabor A, Ferrier E, Jacquelin E, Hamelin P. Analysis and modelling of the in-plane shear behaviourof hollow brick masonry panels. Constr Build Mater 2006;20:308–21.
[19] Gabor A, Bennani A, Jacquelin E, Lebon F. Modelling approaches of the in-plane shear behaviour of of unreinforced and FRP strengthened masonry panels. Compos Struct 2006; 74:277–88.
[20] Valluzzi MR, Tinazzi D, Modena C. Shear behavior of masonry panels strengthened by FRP laminates. Constr Build Mater 2002;16:409–16.
[21] Santa María H, Alcaino P, Luders C. Experimental response of masonry walls externally reinforced with carbon fiber fabrics. In: Proceedings of the 8th US national conference on earthquake engineering, San Francisco, CA, USA, 2006.
[22] Buchan P, Chen J. Blast resistance of FRP composites and polymer strengthened concrete and masonry structures—a state-of-the-art review. Compos Part B—Eng 2007;38:509–22.
[23] Oliveira DV, Basílio I, Lourenço PB. FRP strengthening of masonry arches towards an enhanced behaviour. In: Proceedings of the third international conference on bridge maintenance, safety and management-bridge maintenance, safety, management, life-cycle performance and cost 2006. p.1067–8.
[24] Donnelly E. Keeping a wrap on it. Concrete (London) 2006;40(4):33–4.
[25] Panichkov D, Rangelova F. The FRPs upgrade the masonry walls—an experimental investigation. In: Proceedings, annual conference—Canadian Society for Civil Engineering, 2005: FR-161-1-FR-161-7.
[26] Rangelova F, Panichkov D, Nikolova B. Composite repair technology—constructive solution on masonry wall's strengthening (experimental study). In: Proceedings of the international SAMPE symposium, vol. 50 2005. p. 173–8.
[27] Alessandro B, Ottavia C. Stress analysis of masonry vaults and static efficacy of FRP repairs. Int J Solids Struct 2007;44:8028–56.
[28] Willis CR, Yang Q, Seracino R, Griffith MC. Damaged masonry walls in two-way bending retrofitted with vertical FRP strips. Constr Build Mater 2009;23:1591–604.
[29] CEN. European norm for methods of test for masonry—Part 3: Determination of initial shear strength. prEN 1052-3, 1999.
[30] Abdou L, Saada R, Meftah FY Merbaki A. Experimental and numerical study of the brick–mortar interface. In: Proceedings of the XXI ICTAM 2004, Warsaw, Poland.
[31] Luccioni B, Oller S, Danesi R. Coupled plastic-damaged model. Comput Method Appl Mech Eng 1996;129:81–9.
[32] Luccioni B, Rougier V. A plastic damage approach for confined concrete. Comput Struct 2005;83:2238–56.
[33] Luccioni B. Constitutive model for fiber reinforced composite laminates. J Appl Mech—Trans ASME 2006;73(6):901–10.
[34] Toledo M, Nallim L, Luccioni B. A micro-macromechanical approach for composite laminates. Mech Mater 2008;40:885–906.
[35] Luccioni B, Martín P. Modelo elastoplástico para materiales ortótropos. Rev Int Mét Numér Dis Cálc Ing 1996;13(4):603–14.
[36] Betten J. Application of tensor functions to the formulation of yield criteria for anisotropic materials. Int J Plasticity 1988;4:29–46.
[37] Luccioni B, Oller S, Danesi R. Plastic damaged model for anisotropic materials. Appl Mech Am 1995;I:124–9.
[38] Oller S, Botello S, Miquel M, Oñate. Anisotropic elasto-plastic model based on an isotropic formulation. Eng Comput 1995;12:245–62.
[39] Luccioni B, Martín PE. Modelo elastoplástico para materiales ortótropos. Rev Int Mét Num Dis Cálc Ing 1997;13(4):603–14.
[40] Car E, Oller S, Oñate E. A large strain plasticity model for anisotropic composite material application. Int J Plasticity 1999;17(11):1437–63.
[41] Oller S, Car E, Lubliner J. Definition of a general implicit orthotropic yield criterion. Comput Method Appl Mech Eng 2003;192:895–912.